



Effect of bismuth titanate on the properties of potassium sodium niobate-based ceramics

Henry E. Mgbemere, Theddeus T. Akano & Gerold. A. Schneider

To cite this article: Henry E. Mgbemere, Theddeus T. Akano & Gerold. A. Schneider (2017) Effect of bismuth titanate on the properties of potassium sodium niobate-based ceramics, *Journal of Asian Ceramic Societies*, 5:1, 49-55, DOI: [10.1016/j.jascer.2016.12.006](https://doi.org/10.1016/j.jascer.2016.12.006)

To link to this article: <https://doi.org/10.1016/j.jascer.2016.12.006>



© 2017 The Ceramic Society of Japan and
the Korean Ceramic Society



Published online: 20 Apr 2018.



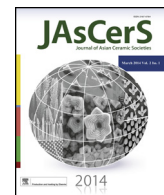
Submit your article to this journal



Article views: 31



View Crossmark data



Full Length Article

Effect of bismuth titanate on the properties of potassium sodium niobate-based ceramics

Henry E. Mgbemere ^{a,c,*}, Theddeus T. Akano ^b, Gerold A. Schneider ^c^a Department of Metallurgical and Materials Engineering, University of Lagos Akoka, Lagos Nigeria, Nigeria^b Department of Systems Engineering, University of Lagos Akoka, Lagos Nigeria, Nigeria^c Hamburg University of Technology, Institute of Advanced Ceramics, Denickestrasse 15, D-21073 Hamburg, Germany

ARTICLE INFO

Article history:

Received 28 October 2016

Received in revised form

12 December 2016

Accepted 26 December 2016

Available online 7 January 2017

Keywords:

High-throughput experimentation

(K_xNa_{1-x})NbO₃ ceramics

Ferroelectrics

Piezoelectrics

ABSTRACT

The effect of modifying the properties of KNN-based ceramics with Bi₂Ti₂O₇ (BiT) been investigated in this work. The density measurements show that additions of BiT to the samples slightly increase the density values. Scanning electron microscope images of the samples indicate that the average sizes of the grains decrease with BiT addition while the volume of pores increase. X-ray diffraction results show that for (K_{0.5}Na_{0.5})NbO₃ based samples, a transformation from orthorhombic to pseudo-cubic phase is observed. For both K_{0.48}Na_{0.48}Li_{0.04}(Nb_{0.9}Ta_{0.1})O₃ and K_{0.48}Na_{0.48}Li_{0.04}(Nb_{0.86}Ta_{0.1}SB_{0.04})O₃-based compositions, the phase transition is from an orthorhombic-tetragonal coexistence to a tetragonal structure dominated phase coexistence.

The dielectric constant, dielectric loss and resistivity values of the samples increase slightly with BiT addition. Good hysteresis curves are obtained in (K_{0.5}Na_{0.5})NbO₃-based samples only at low BiT amounts. Remnant polarization values between 9 μC/cm² and 25 μC/cm² are obtained for K_{0.48}Na_{0.48}Li_{0.04}(Nb_{0.9}Ta_{0.1})O₃ and K_{0.48}Na_{0.48}Li_{0.04}(Nb_{0.86}Ta_{0.1}SB_{0.04})O₃-based samples. With the exception of KNNLT samples where the d³³ values increase from 203 ± 7 pm/V at 0 mol% to 275 ± 6 pm/V at 0.35 mol%, the d³³ values of the samples gradually decrease with increasing BiT content. This work shows that to obtain good properties for KNN-based ceramics, only very small amounts of BiT are required.

© 2017 The Ceramic Society of Japan and the Korean Ceramic Society. Production and hosting by Elsevier B.V. This is an open access article under the CC BY-NC-ND license (<http://creativecommons.org/licenses/by-nc-nd/4.0/>).

1. Introduction

Lead Zirconate Titanate (PZT) based piezoelectric ceramics are the materials of choice in the manufacture of actuators and other electromechanical devices but increasing awareness of the hazards due to Pb²⁺ and legislation has prompted the search for possible replacement materials [1]. Several lead-free piezoelectric ceramics compositions with promising properties compared to the PZT do exist and their piezoelectric properties are being engineered to compare with those from lead-based ceramics [2–6]. (K_xNa_{1-x})NbO₃ (KNN)-based piezoelectric ceramics are among the leading lead-free piezoelectric ceramics which have the potential to replace PZT ceramics [7–10].

KNN in its pure form is difficult to synthesize and has low piezoelectric properties [11–13]. Other elements are therefore introduced in the form of dopants to improve its sinterability, piezoelectric and electromechanical properties. Ahn and Schulze, showed that the addition of small amounts of Ba to KNN leads to improvement in density although with little changes in the electrical properties [14]. Addition of between 2 and 3 mol% of (Bi_{0.5}K_{0.5})TiO₃ to KNN has also been shown to result in a phase change from orthorhombic to tetragonal symmetry with increased piezoelectric and electromechanical properties [15]. The addition of (Bi_{0.5}Na_{0.5})TiO₃ to KNN resulted in a similar result [16]. Addition of BiScO₃ to KNN showed that the phase present is orthorhombic when the dopant amount is <1.5 mol% and pseudo-cubic when it is >2 mol%. The resulting piezoelectric properties are better when compared to the undoped form [17].

Lead-free piezoelectric ceramics are now being tested in potential applications such as ultrasonic transducers [18], actuators [19] with excellent electroacoustic performances comparable to those of commercial PZT ceramics [18,20].

* Corresponding author at: Department of Metallurgical and Materials Engineering, University of Lagos Akoka, Lagos Nigeria.

E-mail addresses: hmgbemere@unilag.edu.ng, takano@unilag.edu.ng (T.T. Akano), g.schneider@tuuh.de (Gerold.A. Schneider).

There is need to screen as fast as possible new ceramic compositions which may have better properties while also limiting both raw material usage and the processing time involved. This is the driving force for the use of the high-throughput process in the synthesis of bulk ceramics [21]. High-throughput experimentation (HTE) uses miniaturization, robotics and parallel techniques to increase the productivity of the research process while the screening/analysis is the use of parallel assay to rapidly assess the activity of the samples produced through this process [22]. It has been employed for long in pharmaceutical research where several thousands if not millions of different compositions need to be tested in order to get the required drug [23]. It has recently been gradually used in other areas of materials research like polymer [24], catalysts [25] and thin film ceramics [26]. Its application to the making of bulk ceramics [21,26] has however been limited because of the difficulty to reproduce them since only small amounts of powders are normally used. Certain properties like piezoelectric charge coefficients are better characterized using ceramics in their bulk form and so our HTE method from dry powders has been adapted for bulk ceramics processing.

Reliability of the properties obtained from KNN based ceramics is also of great concern for instance their temperature stability [27] and bipolar fatigue behaviors [28]. These considerations need to be studied more possibly with HTE methods.

The objective of this work is to use high-throughput experimentation to study the effect of adding small amounts of $\text{Bi}_2\text{Ti}_2\text{O}_7$ on the microstructure, dielectric and piezoelectric properties of KNN ceramics. Bismuth titanate often expressed as $\text{A}_2\text{O}'\text{B}_2\text{O}_6$, is a pyrochlore which contains A-cations which have active lone pairs and exhibit disorder in the $\text{A}_2\text{O}'$ network often [29]. It belongs to the Aurivillius family of compounds with a layered structure in which n perovskite-like $(\text{A}_{n-1}\text{B}_n\text{O}_{3n+1})^{2-}$ blocks alternate with $(\text{Bi}_2\text{O}_2)^{2+}$ layers. It is ferroelectric with Curie temperature ($T_C = 675^\circ\text{C}$) and remnant polarization ($P_r = 50 \mu\text{C}/\text{cm}^2$) along the main polar crystallographic a -axis [30]. It is reported to also exhibit high permittivity and low leakage current [29]. Although BiT has a pyrochlore structure, its choice as a dopant in this study is based on the similarity in properties between the element bismuth and lead. The positive effect of PbTiO_3 on the piezoelectric properties in the well-studied $\text{Pb}(\text{Zr}_x\text{Ti}_{1-x})\text{O}_3$ system was also taken into consideration.

2. Experimental procedure

2.1. Sample preparation

Li_2CO_3 , Na_2CO_3 , K_2CO_3 , (99 +%) Nb_2O_5 , Sb_2O_3 and Ta_2O_5 (99.9%), (ChemPur GmbH, Karlsruhe, Germany), and $\text{Bi}_2\text{Ti}_2\text{O}_7$ (99 +%) (Certronic Ind. Com. Ltda, Brasil) were used as starting powders. The powders were dried at 200°C for 4 h to remove any retained moisture prior to dosing. Dosing of the powders was done using a dosing robot (ChemSpeed Technologies, Switzerland) whose operating principles has been explained in a previous article [31].

1100 mg of $1 - x[(\text{K}_{0.5}\text{Na}_{0.5})\text{NbO}_3] - x\text{BiT}$ [KNN-BiT], $1 - x[(\text{K}_{0.48}\text{Na}_{0.48}\text{Li}_{0.04})(\text{Nb}_{0.9}\text{Ta}_{0.1})\text{O}_3] - x\text{BiT}$ [KNNLT-BiT], and $1 - x[(\text{K}_{0.48}\text{Na}_{0.48}\text{Li}_{0.04})(\text{Nb}_{0.86}\text{Ta}_{0.1}\text{Sb}_{0.04})\text{O}_3] - x\text{BiT}$ [KNNLST-BiT] were dosed and then dry-mixed using a speed mixer (DAC-150 FVZ Hauschild Engineering, Germany) operating at 1600 rpm for 1 min. $\text{Bi}_2\text{Ti}_2\text{O}_7$ powder was added to the KNN variants from 0 mol% to 0.5 mol% with 0.05 mol% steps. Milling of the powders was done in a HTE compatible planetary mill where 16 different compositions were milled at a time. A milling speed of 200 rpm for 3 h using ethanol as solvent and 3 mm diameter zirconia balls as grinding media was used. The solution was dried in vacuum to reduce the influence of moisture and later calcined in a tube furnace at 850°C for 4 h. The milling process was repeated to homogenize the pow-

ders and reduce their average particle size. The powders were put in an in-house made silicone mold and shaped using a cold isostatic press at 300 MPa for 2 min to obtain pellets of approximately 8.0 mm diameter and 2.5 mm thickness. Sintering was carried out in air between 1080°C and 1130°C for 1 h. For $0 \leq x \leq 0.25$, the sintering temperature was 1080°C for KNN-BiT and KNNLT-BiT respectively, 1100°C for KNNLT-BiT compositions. For $0.3 \leq x \leq 0.5$, the temperature used was 1090°C for KNN-BiT and KNNLT-BiT respectively and 1130°C for KNNLT-BiT compositions.

2.2. Sample characterization

The densities of the samples were determined using Archimedes method and the samples were ground and subsequently polished for characterization. The diameter and thickness of the samples after mechanical polishing are approx. 1.4 mm thickness by 7.4 mm diameter. The crystal structure of the sintered samples were examined using an X-ray diffraction (XRD) (D8 Discover, Bruker AXS, Karlsruhe, Germany) with $\text{CuK}\alpha$ radiation ($\lambda = 1.54056 \text{\AA}$), Göbel mirror and General Analysis Diffraction Detection System (GADDS). Six separate measurements were made on selected locations on the surface of the sample between 20° and 56° to examine sample homogeneity. The samples were thermally etched at a temperature of 900°C for 30 min at a heating and cooling rate of $3^\circ\text{C}/\text{min}$ and $10^\circ\text{C}/\text{min}$ respectively. Microstructural examination was done using a Scanning Electron Microscope (LEO 1530 FESEM, Gemini/Zeiss, Oberkochen, Germany) while the average grain size was determined using the Mean Intercept Length Method from at least 6 different lines on the SEM image. Silver paint acting as electrodes was applied on both surfaces of the samples for resistance, dielectric and piezoelectric property measurements. Polarization hysteresis measurements were carried out using the standard Sawyer–Tower circuit and a complete dipolar hysteresis measurement was performed in 200 s. Unipolar strain hysteresis measurements were performed on the sample to determine the high signal piezoelectric charge coefficient values for the samples. An external electric field of 2 kV/mm was applied on the samples for the hysteresis measurements

3. Results and discussion

When a material like $\text{Bi}_2\text{Ti}_2\text{O}_7$ or any other compound is used as a dopant, it is the individual elements present that influence the properties of the doped material. The estimation of the position of the individual dopant elements in the lattice of KNN ceramics is based in principle on the ionic radius, coordination number and valence states of the elements. Bismuth in its natural state is multivalent with +3 and +5 valence states, ionic radius of 1.03\AA and 0.76\AA respectively and a coordination number of 6. Based on the chemical composition, the +3 state is more likely to be present. Titanium is also multivalent with +2, +3 and +4 valence states and for a coordination number of 6; the ionic radius is 0.86\AA , 0.67\AA and 0.605\AA respectively. The +4 valence state is also believed to be present based on the composition.

The A-site of the perovskite lattice in KNN ceramics contains Na and K with +1 valence states. The coordination number of the A-site of the perovskite lattice is 12 and so the corresponding ionic radius is 1.39\AA and 1.64\AA . The B-site on the other hand has a coordination number of 6 and for Niobium which sits on this site; the coordination numbers are 0.68\AA and 0.64\AA for valence states of +4 and +5 respectively. Based on the coordination number alone, the elements in both dopants are expected to enter the B-site of the lattice but if the ionic radius is taken into consideration, Bi can also enter the A-site of the lattice. It is therefore difficult to describe exactly the influence of each dopant element on the properties of

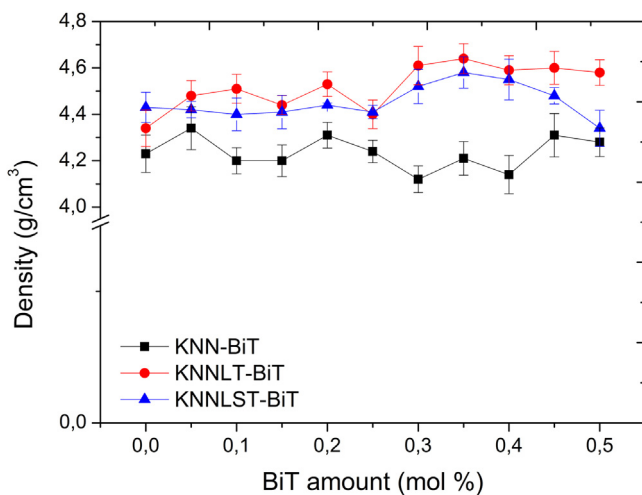


Fig. 1. Bulk density values for $(K_{0.5}Na_{0.5})NbO_3$, $(K_{0.48}Na_{0.48}Li_{0.04})(Nb_{0.9}Ta_{0.1})O_3$ and $(K_{0.48}Na_{0.48}Li_{0.04})(Nb_{0.86}Ta_{0.1}Sb_{0.04})O_3$ ceramics modified with $Bi_2Ti_2O_7$.

the KNN-based ceramics and so the contribution of the dopant as a whole has been adopted for this study.

Our previous study on the doping of KNNLS ceramics with Ti alone indicated lowering of the average grain size, dielectric constant, piezoelectric coefficients while the current density increases by many orders of magnitude [32]. Bismuth has been reported to increase the sintering temperature, average grain size, piezoelectric charge coefficient with ≤ 0.5 wt.% while the remnant polarization and coercive field are lowered. The sample is made porous with very little amounts of the dopant increasing the tendency to show signs of high leakage current during poling [33,34].

3.1. Density

The bulk density values for all the samples are shown in Fig. 1. Due to the difficulty in sintering all the samples using different temperatures, the knowledge of the composition and amount of the elements that make up the ceramics was used to estimate sintering temperatures that are appropriate for a range of compositions. Based on this concept, four different sintering temperatures are used to obtain the best possible density values for the samples. The bulk density values for KNN compositions with BiT addition are ~ 4.2 g/cm³. Compared to the bulk density values of samples with similar compositions produced using conventional methods, there is no significant difference in the reported values [11,35].

The increasing addition of up to 0.25 mol% BiT to KNNLT ceramics led to a gradual increase in the obtained density values from 4.34 ± 0.08 g/cm³ to 4.6 ± 0.08 g/cm³. This increase shows how small amounts of the dopant with the appropriate sintering temperature can improve the density values. Attempts made to sinter some of the samples at temperatures above 1130 °C resulted in poorly sintered samples with high porosity and so the process was discontinued. For the KNNLST compositions, when up to 0.25 mol% BiT was added, the density values remain unchanged at 4.43 ± 0.06 g/cm³. With more than 0.25 mol% however, the density of the samples slightly increases to 4.5 ± 0.07 g/cm³ at 0.35 mol% and gradually decreases with more dopant addition. This is similar to the density results that have been reported in the literature for samples with related compositions [36,37].

3.2. Phase determination

The X-ray diffraction patterns for all the samples are shown in Fig. 2. The rule of thumb in the qualitative determination of the

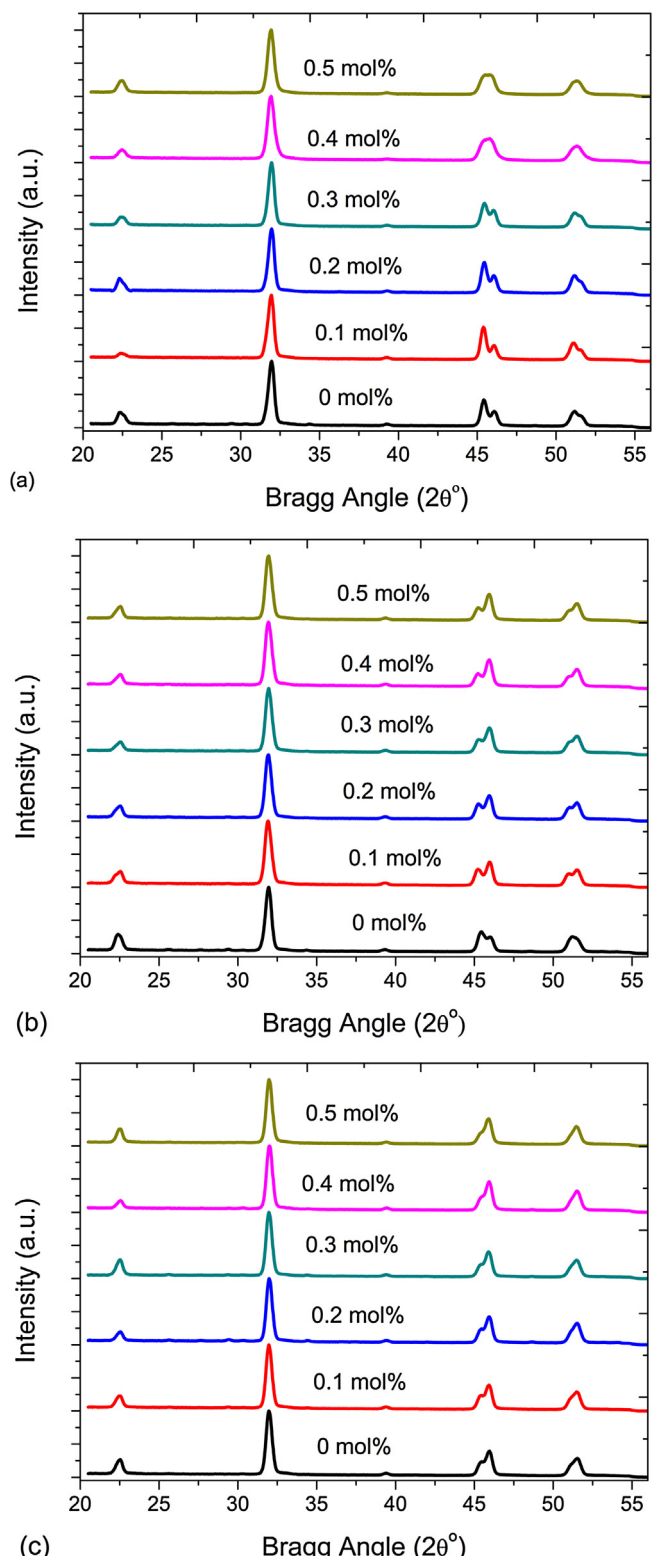


Fig. 2. X-ray diffraction patterns for (a) $(K_{0.5}Na_{0.5})NbO_3$ -BiT, (b) $(K_{0.48}Na_{0.48}Li_{0.04})(Nb_{0.9}Ta_{0.1})O_3$ -BiT and (c) $(K_{0.48}Na_{0.48}Li_{0.04})(Nb_{0.86}Ta_{0.1}Sb_{0.04})O_3$ -BiT ceramics.

type of phase present in any material (especially for those with orthorhombic and tetragonal phases) is by using the pseudo-cubic 002 and 200 reflections. When the ratio between the two reflections is 2, the phase is accepted to be orthorhombic, when it is 0.5, it is tetragonal and when it is approximately equal to 1, the

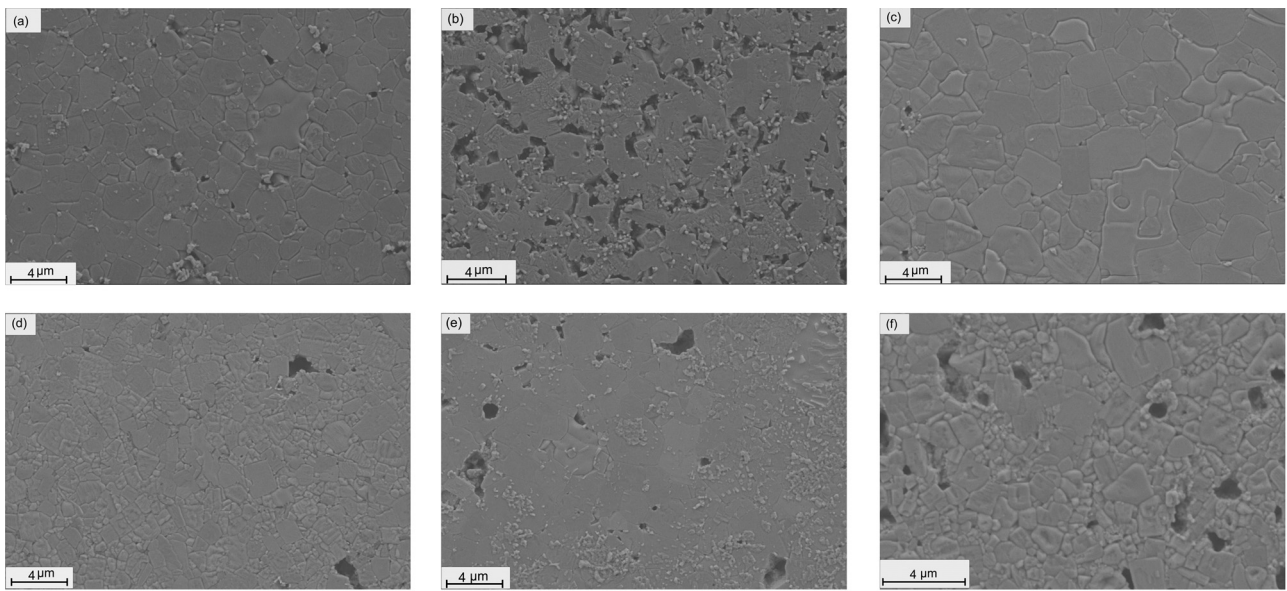


Fig. 3. SEM image of the polished surface of (a) KNN-0 mol% BiT sintered at 1080 °C. (b) KNN-0.5 mol% BiT sintered at 1090 °C (c) KNNLT-0 mol% BiT sintered at 1100 °C (d) KNNLT-0.5 mol% BiT sintered at 1130 °C (e) KNNLT-0 mol% BiT sintered at 1080 °C (f) KNNLT-0.5 mol% BiT sintered at 1090 °C.

two phases are said to coexist with each other [38]. For KNN compositions (Fig. 2a), the unmodified sample has an orthorhombic phase and this phase is present up to 0.3 mol% BiT addition. With doping amounts between 0.35 mol% and 0.5 mol%, the two-phase orthorhombic-tetragonal phase coexistence is observed. Similar results have been reported in the literature for KNN ceramics of like compositions obtained from conventional methods [39].

A previous report in the literature from conventional method for KNNLT ceramics indicates a two-phase coexistence for this composition [38]. In the KNNLT compositions shown in Fig. 2b, the unmodified sample appears to be more orthorhombic than tetragonal. The addition of BiT to the ceramics transforms the phase present to be more tetragonal than orthorhombic. This is an indication that the presence of BiT in the sample stabilizes the tetragonal phase. The diffraction patterns for the KNNLT compositions (Fig. 2c) show that in the unmodified sample, the phase present is more tetragonal than orthorhombic. The addition of BiT up to 0.5 mol% did not have a significant effect on the structure of the samples as the tetragonal phase is retained. A look at the density values of the KNNLT samples shows that there is no significant change in the values with doping.

3.3. Microstructural analysis

The scanning electron microscope images of the polished and thermally etched samples modified with 0 mol% and 0.5 mol% of BiT respectively are shown in Fig. 3. In the unmodified KNN sample (Fig. 3a), the grain size distribution is more or less unimodal with a few pores at the grain boundaries. The calculated average grain size of the micrograph is $2.6 \pm 1.1 \mu\text{m}$. When 0.5 mol% of BiT (Fig. 3b) is added to KNN ceramics, interconnected pores which are mainly at the grain boundary region could be observed. The sizes of the grains are also smaller compared to those of the unmodified sample with an average size of $2.1 \pm 0.7 \mu\text{m}$. A possible reason for the higher volume of pores could be that Bi segregates to the grain boundaries and because it has a high vapor pressure at elevated temperatures, vaporizes during sintering leaving pores where it once was. The density values of the 0 and 0.5 mol% BiT doped samples are similar because the higher porosity in the later is compensated by the smaller size of the grains.

For the KNNLT composition without BiT addition in Fig. 3c, a unimodal grain size distribution is observed with little or no pores at the grain boundaries. An average grain size of $2.8 \pm 1.1 \mu\text{m}$ is obtained. When 0.5 mol% of BiT is added (Fig. 3d) however, the average grain size decreases to $1.7 \pm 0.6 \mu\text{m}$ with few, isolated pores seen at the grain boundary. This decrease in the average size of the grains translates to a slightly higher density value for the 0.5 mol% doped sample.

The KNNLT composition without BiT modification is shown in Fig. 3e. There are few pores at the grain boundaries and the size distribution is arguably unimodal with a calculated average grain size of $2.9 \pm 1.0 \mu\text{m}$. When 0.5 mol% of BiT is added to the sample (Fig. 3f), few large grains surrounded by many small grains are obtained. When the size of the grains are calculated as though they are unimodal, the calculated average size is $1.7 \pm 0.6 \mu\text{m}$.

In all the BiT-modified samples, their average grain sizes are smaller than in the unmodified samples and this implies that BiT is a grain growth inhibitor in KNN-based ceramics. A possible mechanism through which this occurs is by grain boundary pinning which inhibits the growth of the grains [8,40].

3.4. Dielectric properties

The dielectric constant and dielectric loss values for the samples measured at room temperature and at a frequency of 1 kHz are shown in Fig. 4a and b respectively. The addition of BiT to all the KNN-based ceramics resulted in an increase in the obtained permittivity values. The dielectric constant values of the KNN and KNNLT samples increase by 22% and 63% respectively after addition of 0.5 mol% BiT while that of KNNLT samples increase by 18% with the addition of 0.45 mol% BiT. The increase in the density of KNNLT compositions with doping is believed to have contributed to the improved dielectric constant values. Of the three KNN-based ceramics, KNN compositions have the lowest dielectric constant values followed by KNNLT compositions and finally KNNLT compositions. It has been reported that with isovalent element substitutions in KNN ceramics, both the sinterability and properties of the ceramics is improved [2,7,41]. The contributions to dielectric polarization in this case are possibly by electron shift within the molecules, the rotating dipolar molecules and/or the changing of ion places in the lattice. The addition of BiT has a positive effect on the

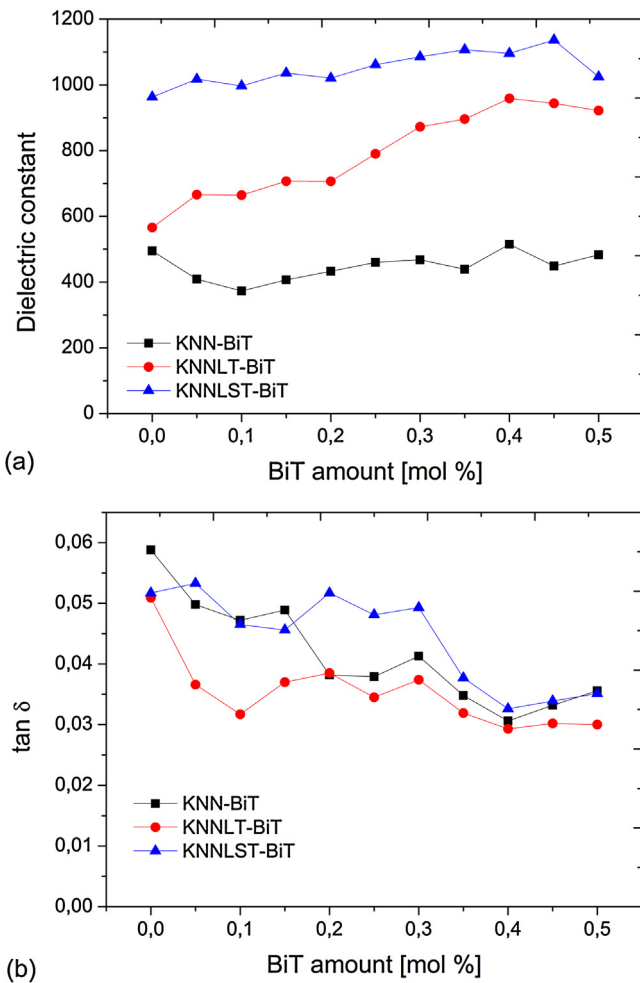


Fig. 4. (a) Dielectric constant values for KNN-BiT, KNNLT-BiT and KNNLST-BiT measured at 1 kHz and at room temperature. (b) Dielectric loss ($\tan \delta$) values measured at 1 kHz.

dielectric constant possibly because the main contribution to the dielectric constant in the sample at low frequency is from space charges [42,43]. The high space charges may be due to oxygen ion vacancies existing in the layer structure as a result of the doping.

The dielectric loss of a material is a measure of the energy dissipation and for the KNN-based compositions; it generally decreases with increasing BiT amount. The dielectric loss values for all the samples are between 0.025 and 0.06 which is comparable to values obtained for similar compositions obtained through the conventional synthesis method [11,12]. KNNLST compositions have the highest loss values followed by KNN compositions with KNNLT compositions having the least loss values. The grain sizes of all the samples generally decrease while the density either increases or remains constant with BiT addition and this could be why energy dissipation is lowered.

3.5. Resistivity

The resistivity values for the samples as a function of the amount of BiT added are shown in Fig. 5. A trend is observed in the resistivity values for all the samples where they increase in the following order: from KNN compositions to KNNLT compositions and lastly to KNNLST compositions. The resistivity values for each composition remain virtually unchanged with the addition of BiT up to 0.25 mol%. The resistivity values for all the samples however

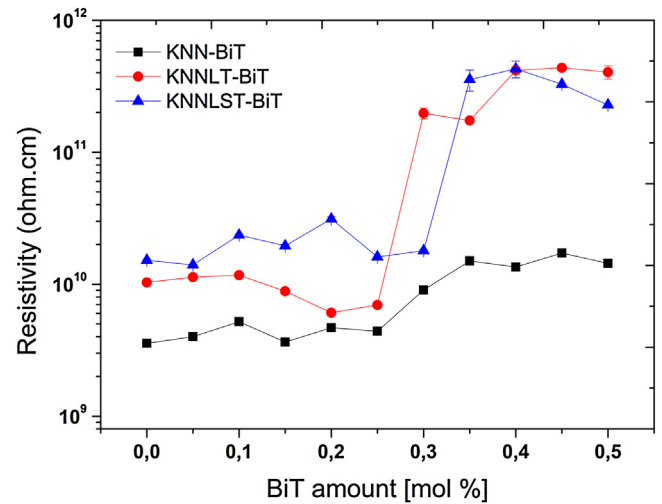


Fig. 5. Resistivity values for KNN-BiT, KNNLT-BiT and KNNLST-BiT compositions measured at room temperature.

increase with more than 0.25 mol% BiT. For KNN compositions, the increase is from $\sim 3 \times 10^9 \Omega \text{ cm}$ for doping below 0.25 mol% BiT to $\sim 10^{10} \Omega \text{ cm}$ for doping above 0.25 mol% BiT. For KNNLT and KNNLST compositions, the resistivity values increase by one order of magnitude from $\sim 10^{10} \Omega \text{ cm}$ for doping below 0.25 mol% BiT to $\sim 3 \times 10^{11} \Omega \text{ cm}$. The lower average grain sizes of the doped samples possibly due to their pinning action at the grain boundaries is believed to have led to a decrease in the mobility of the charge carriers. It is also possible that discontinuities in the samples resulted in some form of blocking at the electrode which trapped the charge carriers.

3.6. Hysteresis measurement

The polarization hysteresis curves for the samples as a function of the applied electric field are shown in Fig. 6. The hysteresis loops for KNN compositions are shown in Fig. 6a and they indicate that good hysteresis curves could not be obtained for most of the samples. The remnant polarization (P_r) gradually decreases with increasing amount of BiT while the coercive field E_C did not change significantly. The phase transformation from orthorhombic to pseudo-cubic with more BiT addition, the presence of pores in some of the SEM images and low density are possibly the reasons for the high leakage current and subsequent egg-shaped nature of some of the curves. Acceptable polarization hysteresis curves could not be obtained for all the KNNLT compositions (Fig. 6b) and the E_C values decrease with increasing amount of BiT. When small BiT amounts are added to KNN ceramics, saturation polarization P_S could not be obtained for the samples with 20 kV/cm while the P_r is $\sim 25 \mu\text{C}/\text{cm}^2$. As more amounts are added however, P_S could be attained but the P_r value reduces to $\sim 9 \mu\text{C}/\text{cm}^2$. Although the density values increase and the diffraction patterns remained weakly tetragonal, few isolated pores on the micrograph could explain why there is moderately high leakage current during the measurement.

The hysteresis curves for KNNLST compositions as a function of the applied field is shown in Fig. 6c. Good polarization curves are obtained for almost all the KNNLST compositions. As the amount of BiT added increases, full saturation polarization could no longer be achieved a field of 20 kV/cm and more additions led to a decrease in the P_r but the E_C for most of the samples remains between 10 and 12 kV/cm. There is however no clearly defined trend with sample modification. The good nature of the loops obtained here can be

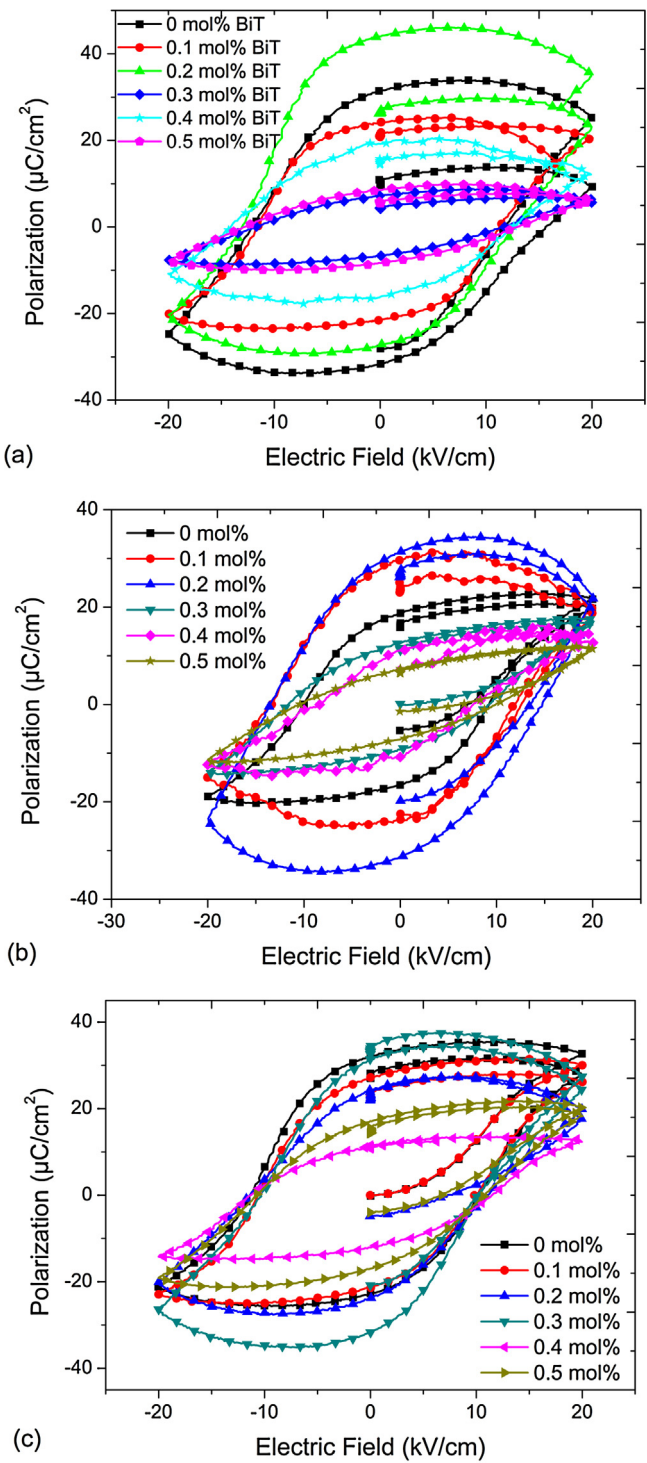


Fig. 6. Polarization hysteresis curves for (a) KNN-BiT ceramics, (b) KNNLT-BiT ceramics (c) KNNLST-BiT ceramics.

traced to the base $(\text{KNaLi})(\text{NbTaSb})\text{O}_3$ composition which has been reported have one of the best piezoelectric properties [7].

3.7. Piezoelectric charge coefficient

Unipolar strain hysteresis measurements are normally used to determine the high signal piezoelectric charge coefficient (d^{*}_{33}) values for samples with piezoelectric properties. A representative unipolar strain hysteresis curves for KNN, KNNLT and KNNLST compositions doped with BiT is shown in Fig. 7a. The d^{*}_{33} values as

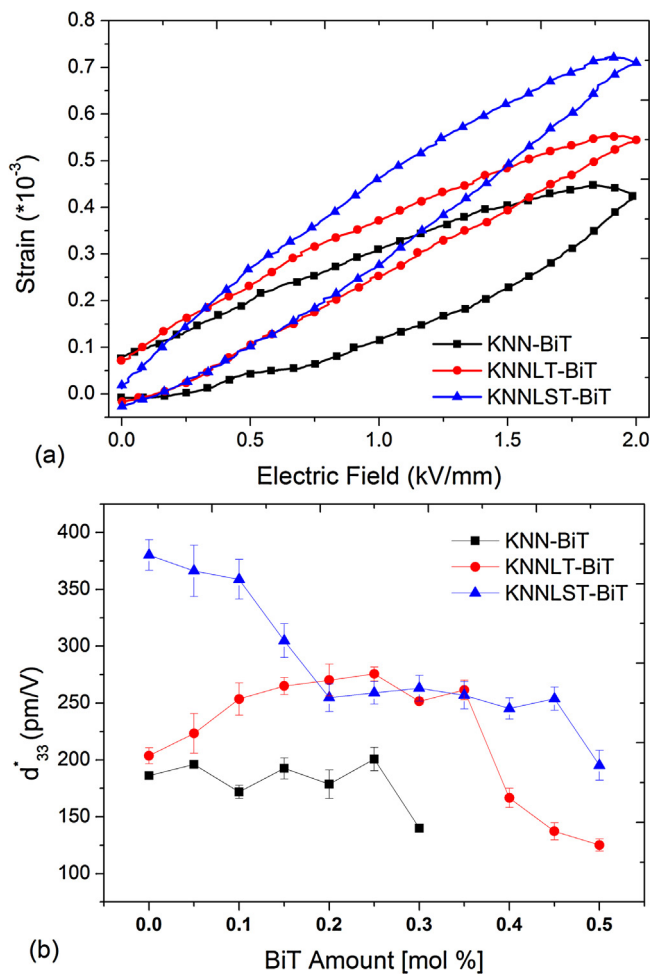


Fig. 7. (a) Representative unipolar strain hysteresis curves for KNN, KNNLT and KNNLST compositions modified with BiT and (b) high signal piezoelectric charge coefficient (d^{*}_{33}) values as a function of the amount of BiT for KNN, KNNLT and KNNLST ceramics.

a function of BiT amount for the samples are shown in Fig. 7b. For KNN compositions, no significant change in the d^{*}_{33} values is observed when BiT is added. Due to high leakage currents during measurements, no value is recorded for KNN compositions when more than 0.3 mol% of BiT is added. This is also reflected in the hysteresis curves which show signs of charging and in the dielectric properties where the values increase only slightly with doping. For KNNLT compositions, the addition of up to 0.35 mol% BiT resulted in an increase in the d^{*}_{33} values but with higher amounts of BiT, the d^{*}_{33} values decrease. For KNNLST compositions, a gradual decrease in the d^{*}_{33} values with increasing BiT addition is observed. The d^{*}_{33} values however remained constant at $\sim 250 \text{ pm/V}$ with BiT additions of between 0.2 mol% and 0.45 mol%. The pseudo-cubic nature of the diffraction patterns, the interconnected pores and poor hysteresis loops can be traced to be the cause of the low d^{*}_{33} values for KNN compositions with increasing BiT amounts.

For KNNLT compositions, the relatively improving d^{*}_{33} values with BiT addition up to 0.3 mol% can be related to the increase in the density, dielectric constant and resistivity respectively. As these values begin to decrease, the d^{*}_{33} also deteriorate. Although the diffraction patterns are tetragonal, density values improve and relatively good polarization hysteresis values were obtained with BiT additions, the measured d^{*}_{33} values decrease. This can be explained by the hard piezoelectric properties which the dopant imparts to an otherwise soft piezoelectric ceramic.

4. Conclusion

KNN-based ferroelectric ceramics modified with $\text{Bi}_2\text{Ti}_2\text{O}_7$ has been synthesized using high-throughput experimentation method. Addition of the dopant resulted in a slight increase in the obtained density values. Transformations in the X-ray diffraction patterns are observed with the addition of BiT to the KNN-based compositions. With BiT addition up to 0.3 mol%, the phase present in the KNN compositions is predominantly orthorhombic and with more doping, changes to a pseudo-cubic phase. On addition of more than 0.05 mol% of BiT to KNNLT compositions, there is a phase transformation from mainly orthorhombic to mainly tetragonal while for KNNLST compositions, the tetragonal phase is retained with up to 0.5 mol% of BiT added to the samples.

The SEM images without BiT addition show a unimodal grain size distribution with few pores at the grain boundaries. However, on addition of BiT to the samples, the average grain size decreases while the volume of pores slightly increases.

The dielectric constant values for all the KNN compositions increase with increasing BiT amounts while the dielectric loss values decrease. For all the samples, the loss tangent was between 0.025 and 0.06. The resistivity values for all the KNN-based samples did not significantly change with up to 0.25 mol% of BiT but increases with increasing BiT content up to 0.5 mol%. Good polarization hysteresis curves are obtained for some of the samples and the remnant polarization values for samples with good hysteresis curves are between $\sim 9 \mu\text{C}/\text{cm}^2$ and $25 \mu\text{C}/\text{cm}^2$. In all cases, increasing the amount of BiT added led to a decrease in the remnant polarization but the E_c is generally between 10–12 kV/cm. There is no significant effect of BiT on the d_{33}^* values (186 pm/V) for KNN compositions but for KNNLT samples, the values increase from $203 \pm 7 \text{ pm/V}$ at 0 mol% up to $275 \pm 6 \text{ pm/V}$ at 0.35 mol%. For KNNLST compositions, the d_{33}^* values decrease from $380 \pm 14 \text{ pm/V}$ at 0 mol% to $195 \pm 13 \text{ pm/V}$ at 0.5 mol%.

Acknowledgment

The authors gratefully acknowledge the financial support from Deutsche Forschungsgemeinschaft (DFG) under the grant: SCHN 372/16:1-2

References

- [1] European Parliament and the Council, Eur. J., 37, 1–9 (2003).
- [2] J. Roedel, W. Jo, K.T.P. Seifert, E.-M. Anton, T. Granzow and D. Damjanovic, J. Am. Ceram. Soc., 92, 1153–1177 (2009).
- [3] M. Hirose, T. Suzuki, H. Oka, K. Itakura, Y. Miyauchi and T. Tsukada, Jpn. J. Appl. Phys., 38, 5561–5563 (1999).
- [4] H. Nagata, N. Koizumi, N. Kuroda, I. Igarashi and T. Takenaka, Ferroelectrics, 229, 273–278 (1999).

- [5] X. Wang, J. Wu, D. Xiao, J. Zhu, X. Cheng, T. Zheng, B. Zhang, X. Lou and X. Wang, J. Am. Chem. Soc., 136, 2905–2910 (2014).
- [6] C.-H. Hong, H.-P. Kim, B.-Y. Choi, H.-S. Han, J.S. Son, C.W. Ahn and W. Jo, J. Materomics, 2, 1–24 (2016).
- [7] Y. Saito, H. Takao, T. Tani, T. Nonoyama, K. Takatori, T. Homma, T. Nagaya and M. Nakamura, Nature, 432, 84–87 (2004).
- [8] H.E. Mgbemere, R.-P. Herber and G.A. Schneider, J. Eur. Ceram. Soc., 29, 1729–1733 (2009).
- [9] N.M. Hagh, B. Jadianian and A. Safari, J. Electroceram., 18, (2007).
- [10] S. Zhang, R. Xia and T.R. Shrout, Appl. Phys. Lett., 91, (2007).
- [11] E. Ringgaard and T. Wurlitzer, J. Eur. Ceram. Soc., 25, 2701–2706 (2005).
- [12] L. Egerton and D.M. Dillon, J. Am. Ceram. Soc., 42, 438–442 (1959).
- [13] H. Birol, D. Damjanovic and S. Nava, J. Am. Ceram. Soc., 88, 1754–1759 (2005).
- [14] Z.S. Ahn and W.A. Schulze, J. Am. Ceram. Soc., 70, C18–C21 (1987).
- [15] R. Zuo, X. Fang and C. Ye, J. Am. Ceram. Soc., 90, 2424–2428 (2007).
- [16] R. Zuo, X. Fang and C. Ye, Appl. Phys. Lett., 90, (2007).
- [17] X. Sun, J. Chen, R. Yu, C. Sun, G. Liu, X. Xing and L. Qiaoz, J. Am. Ceram. Soc., 92, 130–132 (2009).
- [18] M. Bah, F. Giovannelli, F. Schoenstein, C. Brosseau, J.-R. Deschamps, F. Dorvaux, L. Haumesser, E.L. Clezio and I. Monot-Laffez, Ultrasonics, 63, 23–30 (2015).
- [19] K. Wang, F.-Z. Yao, W. Jo, D. Gobeljic, V.V. Shvartsman, D.C. Lupascu, J.-F. Li and J. Rödel, Adv. Funct. Mater., 23, 4079–4086 (2013).
- [20] G.C. Edwards, S.H. Choy, H.L.W. Chan, D.A. Scott and A. Batten, Appl. Phys. A, 88, 209–215 (2007).
- [21] A. Cardin, B. Wessler, C. Schuh, T. Steinkopff and W.F. Maier, J. Electroceram., 19, 267–272 (2007).
- [22] J.N. Cawse, Acc. Chem. Res., 34, 213–221 (2000).
- [23] R.B. v. Dover, L.F. Schneemeyer, R.M. Fleming and H.A. Huggins, Biotechnol. Bioeng. (Comb. Chem.), 61, 217–225 (1999).
- [24] S. Schmatloch and U.S. Schubert, Macromol. Rapid Commun., 25, 69–76 (2004).
- [25] J.-D. Grunwaldt, B. Kimmerle, S. Hannemann, A. Baiker, P. Boye and C.G. Schroer, J. Mater. Chem., 17, 2603–2606 (2007).
- [26] C. Schroeter, B. Wessler and L.M. Eng, J. Eur. Ceram. Soc., 27, 3785–3788 (2007).
- [27] F.-Z. Yao, K. Wang, W. Jo, K.G. Webber, T.P. Comyn, J.-X. Ding, B. Xu, L.-Q. Cheng, M.-P. Zheng, Y.-D. Hou and J.-F. Li, Adv. Funct. Mater., 26, 1217–1224 (2016).
- [28] F.-Z. Yao, E.A. Patterson, K. Wang, W. Jo, J. Rödel and J.-F. Li, Appl. Phys. Lett., 104, 242912 (2014).
- [29] A.L. Hector and S.B. Wiggin, J. Solid State Chem., 177, 139–145 (2004).
- [30] M. Villegas, T. Jardiel, A.C. Caballero and J.F. Fernandez, J. Electroceram., 13, 543–548 (2004).
- [31] T.A. Stegk, R. Janssen and G.A. Schneider, J. Comb. Chem., 10, 274–279 (2008).
- [32] H.E. Mgbemere and G.A. Schneider, Ceram. Int., 41, 13232–13240 (2015).
- [33] H. Du, D. Liu, F. Tang, D. Zhu and Z. Wancheng, J. Am. Ceram. Soc., 90, 2824–2829 (2007).
- [34] Y. Wang, Y. Li, K. Kalantar-zadeh, T. Wang, D. Wang and Q. Yin, J. Electroceram., 21, 1–4 (2007).
- [35] J. Bernard, A. Bencan, T. Rojac, J. Holc, B. Malic and M. Kosec, J. Am. Ceram. Soc., 91, 2409–2411 (2008).
- [36] F. Rubio-Marcos, P. Ochoa and J.F. Fernandez, J. Eur. Ceram. Soc., 27, (13) 4125–4129 (2007).
- [37] J. Fu, R. Zuo, Y. Wu, Z. Xu and L. Liz, J. Am. Ceram. Soc., 91, 3771–3773 (2008).
- [38] H.E. Mgbemere, M. Hinterstein and G.A. Schneider, J. Appl. Crystallogr., 44, 1080–1089 (2011).
- [39] T.A. Skidmore, T.P. Comyn, A.J. Bell, F. Zhu and S.J. Milne, IEEE Trans. Ultrason. Ferroelectr. Freq. Control, 58, 1819–1825 (2011).
- [40] S. Zhang, J.B. Lim, H.J. Lee and T.R. Shrout, IEEE Trans. Ultrason. Ferroelectr. Freq. Control, 56, 1523–1527 (2009).
- [41] H.E. Mgbemere, R. Janssen and G.A. Schneider, J. Adv. Ceram., 4, 282–291 (2015).
- [42] H.S. Shulman, M. Testorf, D. Damjanovic and N. Setter, J. Am. Ceram. Soc., 79, 3124–3128 (1996).
- [43] W.-F. Su and Y.-T. Lu, Mater. Chem. Phys., 80, 632–637 (2003).